EJN European Journal of Neuroscience

FENS Federation of European Neuroscience Societies

European Journal of Neuroscience, Vol. 41, pp. 328–340, 2015 doi:10.1111/ejn.12794

MOLECULAR AND SYNAPTIC MECHANISMS

Synapse formation changes the rules for desensitization of PKC translocation in *Aplysia*

Carole A. Farah,[1,*] Faisal Naqib,[2,*] Daniel B. Weatherill,[1] Christopher C. Pack[1,2] and Wayne S. Sossin[1]
[1]Department of Neurology and Neurosurgery, Montreal Neurological Institute, McGill University, 3801 University Street, Montreal, Quebec H3A 2B4, Canada
[2]Department of Physiology, Montreal Neurological Institute, McGill University, Montreal, Quebec, Canada

Keywords: mathematical modeling, PKA, protein synthesis, serotonin

Abstract

Protein kinase Cs (PKCs) are activated by translocating from the cytoplasm to the membrane. We have previously shown that serotonin-mediated translocation of PKC to the plasma membrane in *Aplysia* sensory neurons was subject to desensitization, a decrease in the ability of serotonin to induce translocation after previous application of serotonin. In *Aplysia*, changes in the strength of the sensory–motor neuron synapse are important for behavioral sensitization and PKC regulates a number of important aspects of this form of synaptic plasticity. We have previously suggested that the desensitization of PKC translocation in *Aplysia* sensory neurons may partially explain the differences between spaced and massed training, as spaced applications of serotonin, a cellular analog of spaced training, cause greater desensitization of PKC translocation than one massed application of serotonin, a cellular analog of massed training. Our previous studies were performed in isolated sensory neurons. In the present study, we monitored translocation of fluorescently-tagged PKC to the plasma membrane in living sensory neurons that were co-cultured with motor neurons to allow for synapse formation. We show that desensitization now becomes similar during spaced and massed applications of serotonin. We had previously modeled the signaling pathways that govern desensitization in isolated sensory neurons. We now modify this mathematical model to account for the changes observed in desensitization dynamics following synapse formation. Our study shows that synapse formation leads to significant changes in the molecular signaling networks that underlie desensitization of PKC translocation.

Introduction

Stimulus timing has a significant impact on memory formation. Stimuli presented over time (spaced training) are superior at generating long-term memories than an equivalent amount of stimulation presented with no interruptions (massed training; Naqib *et al.*, 2012) . The marine mollusk *Aplysia californica* has been extensively used to study the molecular mechanisms underlying memory formation. Behavioral sensitization in *Aplysia*, a form of learned fear, is mediated in part by the increase in strength, or facilitation, of the synapse between the mechanoreceptor sensory neurons and the withdrawal motor neurons that is induced by the release of serotonin (5HT) during learning (Brunelli *et al.*, 1976; Glanzman *et al.*, 1989b; Kandel, 2001; Marinesco *et al.*, 2004) . This facilitation can be recapitulated in cultured sensory–motor neuron synapses (Brunelli *et al.*, 1976; Castellucci & Kandel, 1976). Importantly, in this system spaced stimuli are superior at generating long-term sensitization in the animal and long-term facilitation than are massed stimuli (Sutton *et al.*, 2002).

The timing of stimuli also affects the second-messenger dependency of facilitation. 5HT binds to G-protein-coupled receptors (GPCRs) in *Aplysia* and leads to the activation of protein kinase A (PKA) and protein kinase C (PKC) (Lee *et al.*, 2009; Nagakura *et al.*, 2010). Facilitation seen after massed application requires PKC while facilitation seen after spaced application requires PKA (Sutton *et al.*, 2002; Hu *et al.*, 2006; Jin *et al.*, 2011). PKC becomes activated by translocating from the cytoplasm to the plasma membrane and this translocation is subject to desensitization, a decrease in the ability of 5HT to induce translocation after a previous application of 5HT. In isolated sensory neurons, it was observed that spaced applications of 5HT lead to more desensitization of PKC translocation than do massed applications of 5HT (Farah *et al.*, 2009). Through mathematical modeling and experimental validation, we were able to develop a model to explain the neuron's ability to differentiate between spaced and massed applications of 5HT through competition between distinct proteins produced by either PKA or PKC activation (Naqib *et al.*, 2011).

The previously described findings were observed in isolated sensory neurons. However, it is well known that synapse formation can lead to significant changes in molecular signaling networks due to transcriptional-dependent changes in the proteome. In *Aplysia*, synapse formation leads to changes in the mRNAs that are transported down the processes (Schacher *et al.*, 1999; Hu *et al.*, 2004) and changes in the local translation of these mRNAs (Martin *et al.*, 1997;

Correspondence: W. S. Sossin, as above.
E-mail: wayne.sossin@mcgill.ca

*C.A.F. and F.N. contributed equally to this work.

Received 23 April 2014, revised 15 October 2014, accepted 23 October 2014

© 2014 Federation of European Neuroscience Societies and John Wiley & Sons Ltd

Casadio *et al.*, 1999; Martin, 2004; Sutton & Schuman, 2006; Wang *et al.*, 2009). Here, we find that synapse formation changes the rules for desensitization of PKC translocation and we use mathematical modeling to show that these changes could be explained by differential PKA targets at the synapse and cell body, and changes in the identity of the proteins produced downstream of PKA and PKC.

Materials and methods

Aplysia *cell culture preparation*

Sensory neuron cultures and sensory–motor neuron co-cultures were prepared following published procedures (Zhao *et al.*, 2006; Farah *et al.*, 2008). Adult *A. californica* (76–100 g; University of Miami *Aplysia* Resource Facility, RSMAS, FL, USA) organisms were anesthetized by an injection of 50–100 mL of 400 mM (isotonic) $MgCl_2$. Abdominal and/or pleuropedal ganglia were removed and digested in L15 medium containing 1% protease type IX (Sigma) or 10 mg/mL Dispase II (Roche). L15 medium was purchased from Sigma and supplemented with NaCl, 0.2 M and (in mm) – $MgSO_4$ $7H_2O$, 26; dextrose, 35; $MgCl_2 \cdot 6H_2O$, 27; KCl, 4.7; $NaHCO_3$, 2; $CaCl_2 \cdot 2H_2O$, 9.7; and HEPES, 15; and the pH was adjusted to 7.4. Following digestion, siphon motor neurons (LFS) and tail sensory neurons were isolated and plated in L15 medium containing 50% *Aplysia* hemolymph on MatTek glass-bottomed culture dishes (MatTek Corporation, Ashland, MA, USA) with a glass surface of 14 mm and a coverslip thickness of 0.085–0.13 mm. The dishes were pretreated with poly-L-lysine (molecular weight > 300 000; Sigma). Sensory neurons were manually paired with motor neurons to allow for synapse formation and cells were cultured at 19 °C in a high-humidity chamber.

Plasmid construction and microinjection of plasmid vectors

The enhanced green fluorescent protein (eGFP) PKC Apl II has been described previously (Manseau *et al.*, 2001; Zhao *et al.*, 2006; Farah *et al.*, 2009). Forty-eight to seventy-two hours after isolation, solutions of plasmids in distilled water containing 0.25% fast green were microinjected into sensory neurons from back-filled glass micropipettes. The tip of the micropipette was inserted into the cell nucleus, and short pressure pulses (10–50 ms duration; 20 lb/in^2) were delivered until the nucleus became uniformly green. The cells were incubated for 4–5 h at room temperature and then kept at 4 °C until use.

Confocal microscopy of Aplysia *neurons*

Neurons expressing eGFP-PKC Apl II were imaged on a Zeiss laser-scanning microscope (Zeiss, Oberkochen, Germany) with an Axiovert 200 and a × 40 or ×63 oil-immersion objective with a 25-mW argon laser with 25% laser output. 5HT (10 μM) was added to the dish in L15 medium containing 50% hemolymph. 5HT was washed away with artificial seawater (HEPES, pH 7.5, 10 mM; NaCl, 0.46 M; KCl, 10 mM; $CaCl_2 \cdot 2H_2O$, 11.2 mM; and $MgCl_2 \cdot 6H_2O$, 55 mM). For spaced training, neurons received five applications of 10 μM 5HT (5 min each) at an intertrial interval of 20 min. For massed training, neurons received a single continuous application of 10 μM 5HT for 90 min. All experiments were performed at room temperature (20–23 °C).

Drug treatment

Anisomycin (Sigma), and KT5720 (Calbiochem) were used at concentrations of 50 μM, and were present in the media throughout spaced or massed training. There was no pre-incubation with these drugs prior to 5HT treatment and because of this we erred on the high side of the concentrations that have been used previously. The controls used in all experiments were always performed on the same batch of animals on which the drugs were used.

Image analysis

PKC Apl II translocation was quantified as previously described (Zhao *et al.*, 2006; Farah *et al.*, 2008, 2009; Nagakura *et al.*, 2010; Farah & Sossin, 2011a,b; Naqib *et al.*, 2011; Dunn *et al.*, 2012; Farah *et al.*, 2012). Briefly, the level of PKC Apl II translocation in the cell body was determined by tracing three rectangles at different locations at the plasma membrane and three rectangles at different locations in the cytosol. The width of the membrane rectangles was three to five pixels wide to minimize cytoplasmic contamination, but otherwise the size of the rectangles was not constrained. The first two rectangles were traced at opposite sides of the plasma membrane of the cell and the third at an angle of ~45° to the first and second rectangles. The cytosol rectangles were traced in the areas adjacent to the membrane rectangles. For synapses, the entire membrane and cytoplasm of varicosities that adjoined the motoneuron were traced using NIH Image, and the intensity was measured. The translocation ratio was measured as the average intensity (membrane)/average intensity (cytosol) normalized to the degree of translocation before the addition of pharmacological agents (Post/Pre). In all figures, the control used to normalize the translocations in the presence of a drug is the translocation ratio observed after the first application of 5HT in the presence of that drug. A two-way ANOVA was used to analyse the data except when comparing desensitization during spaced applications of 5HT at the 85-min time point to massed application at the 25 min time point (Fig. 3) where a two-tailed Student's *t*-test was used. All data are presented as means ± SEM.

Mathematical modeling

A mathematical model of the desensitization of PKC Apl II translocation in *A. californica* sensory neurons was constructed in the MATLAB programming environment. The model consists of a system of integro-differential equations with delays, where each equation describes the change in concentration of the proteins PKC Apl II, PKA, Desensitizer (D), Anti-Desensitizer (AD), and of each instance of the signaling complex (S) that consists of the 5HT receptor and the downstream signaling between the receptor and PKC activation. As we are only interested in PKC Apl II translocation occurring between the cytosol and plasma membrane (Farah *et al.*, 2008) a single-compartment model was used.

Two models were developed from the original isolated sensory neuron model, one model describing PKC Apl II translocation in the sensory neuron cell body and one model describing PKC Apl II translocation in the sensory neuron varicosities making contact with a motor neuron. The complete models are depicted in Fig. 6. The colors of this figure correspond to the components of the models. The models were constructed in a sequential manner. First, the components outlined in black and maroon were fitted to data (Farah *et al.*, 2009) at which point the model's parameters were specified and not allowed to change. Following these components' completion, the component outlined in blue was similarly constructed, then the red component and finally the green component. In order to illustrate this sequential construction within the model equations, we have named the parameters according to which component they reside in – A for the black component, B for blue, C for red and D for green.

The most basic component of the model is the translocation of PKC Apl II from the cytosol to the plasma membrane (maroon

© 2014 Federation of European Neuroscience Societies and John Wiley & Sons Ltd

component). This translocation is proportional to the concentration of diacylglycerol (DAG) on the membrane and thus the translocation is given by the following equation:

$$\frac{\mathrm{d}}{\mathrm{d}t}\mathrm{PKC} = k_{\mathrm{DAGp}} \times (S_{\mathrm{ON}} + S_{\mathrm{ADON}}) - k_{\mathrm{DAGd}} \times \mathrm{PKC}, \qquad (1)$$

where k_{DAGp} is the rate of PKC Apl II translocation to the membrane and k_{DAGd} the rate of PKC Apl II removal from the membrane. S_{ON} represents the proportion of S currently in the active state, which is capable of translocating PKC Apl II to the membrane. Similarly $\mathrm{S_{ADON}}$ represents the proportion of $\mathrm{S_{AD}}$ (described below) in the active state. The inactive state of S is given by S_{OFF}, and S_{IN1} is a transition state between S_{ON} and S_{OFF}. S can be transformed into three other states, as will be described next. We require the total amount of S to remain constant by employing the following restriction: $\sum_i S_i = S_{\mathrm{TOT}}$, where i = ON, OFF, IN1, IN2, PKA, AD and D. We scale each S variable by $1/S_{\mathrm{TOT}}$, such that all parameters k_{i}, where i = A1–A5, B1–B2, C1–C2 and D1–D3, will have units/min. We have set $S_{\mathrm{TOT}} = 1$, where we refrain from assigning units to the S variables as we cannot measure the concentrations of PKA or PKC in *Aplysia* neurons in order to accurately define a unit of measure. Furthermore, units are not assigned to any variable with concentration as a possible dimension. This simplification is justified as we have developed a single-compartment model of *Aplysia* sensory neurons to qualitatively describe the dynamics of PKC desensitization. Using non-dimensional variables and parameters allows us to observe important dynamics, such as relative magnitudes of proteins and the time course of S recycling, which allow us to gain insight into the molecular regulatory mechanism involved in the desensitization of PKC translocation.

The following equations describe the rates of change of concentration of the first four S states. CB designates equations pertaining to the cell body model while SYN corresponds to the synapse model. Equations with neither CB nor SYN are common to both models.

$$\frac{\mathrm{d}}{\mathrm{d}t}S_{\mathrm{ON}} = k_{\mathrm{A1}} \times [5\mathrm{HT}] \times S_{\mathrm{OFF}} - k_{\mathrm{A2}} \times S_{\mathrm{ON}}, \qquad (2)$$

$$\begin{aligned}\frac{\mathrm{d}}{\mathrm{d}t}S_{\mathrm{OFF}} = {} & -k_{\mathrm{A1}} \times [5\mathrm{HT}] \times S_{\mathrm{OFF}} + k_{\mathrm{A3}} \times S_{\mathrm{IN1}} + k_{\mathrm{A5}} \times S_{\mathrm{IN2}} + k_{\mathrm{B2}} \\ & \times S_{\mathrm{PKA}} \times \frac{k_{\mathrm{B2a}}^{k_{\mathrm{B2b}}}}{\left(k_{\mathrm{B2a}}^{k_{\mathrm{B2b}}} + \mathrm{PKA}^{k_{\mathrm{B2b}}}\right)} - k_{\mathrm{C1}} \times S_{\mathrm{OFF}} \times \mathrm{AD} + k_{\mathrm{C2}} \\ & \times S_{\mathrm{AD}} \times \frac{k_{\mathrm{C2a}}^{k_{\mathrm{C2b}}}}{k_{\mathrm{C2a}}^{k_{\mathrm{C2b}}} + \mathrm{AD}^{k_{\mathrm{C2b}}}} - k_{\mathrm{B1}} \times \mathrm{PKA} \times S_{\mathrm{OFF}},\end{aligned} \qquad (3-CB)$$

$$\begin{aligned}\frac{\mathrm{d}}{\mathrm{d}t}S_{\mathrm{OFF}} = {} & -k_{\mathrm{A1}} \times [5\mathrm{HT}] \times S_{\mathrm{OFF}} + k_{\mathrm{A3}} \times S_{\mathrm{IN1}} + k_{\mathrm{A5}} \times S_{\mathrm{IN2}} + k_{\mathrm{B2}} \\ & \times S_{\mathrm{PKA}} \times \frac{k_{\mathrm{D2a}}^{k_{\mathrm{D2b}}}}{\left(k_{\mathrm{D2a}}^{k_{\mathrm{D2b}}} + \mathrm{D}^{k_{\mathrm{D2b}}}\right)} - k_{\mathrm{C1}} \times S_{\mathrm{OFF}} \times \mathrm{AD} + k_{\mathrm{C2}} \times S_{\mathrm{AD}} \\ & \times \frac{k_{\mathrm{C2a}}^{k_{\mathrm{C2b}}}}{k_{\mathrm{C2a}}^{k_{\mathrm{C2b}}} + \mathrm{AD}^{k_{\mathrm{C2b}}}} - k_{\mathrm{D1}} \times \mathrm{D} \times S_{\mathrm{OFF}},\end{aligned} \qquad (3-SYN)$$

$$\frac{\mathrm{d}}{\mathrm{d}t}S_{\mathrm{IN1}} = k_{\mathrm{A2}} \times S_{\mathrm{ON}} - (k_{\mathrm{A3}} + k_{A4}) \times S_{\mathrm{IN1}}, \qquad (4)$$

$$\frac{\mathrm{d}}{\mathrm{d}t}S_{\mathrm{IN2}} = k_{\mathrm{A4}} \times S_{\mathrm{IN1}} - k_{A5} \times S_{\mathrm{IN2}}, \qquad (5)$$

where [5HT] represents the concentration of 5HT being applied to the system and is given a standard value of 10 μM during any application of 5HT, k_{A1} represents the rate of transformation of S_{OFF} into S_{ON}, k_{A2} of S_{ON} into S_{IN1}, k_{A3} of S_{IN1} into S_{OFF}, k_{A4} of S_{IN1} into S_{IN2} and k_{A5} of S_{IN2} into S_{OFF}. The additional terms in Eqn (3) refer to the further transformations that S_{OFF} can undergo. Without these additional terms these equations describe the black model in Fig. 3A. The first additional transformation of S_{OFF} is mediated by the catalytic subunit of PKA, where S_{OFF} is converted to S_{PKA}, which has the following equation:

$$\frac{\mathrm{d}}{\mathrm{d}t}S_{\mathrm{PKA}} = k_{\mathrm{B1}} \times \mathrm{PKA} \times S_{\mathrm{OFF}} - k_{\mathrm{B2}} \times S_{\mathrm{PKA}} \times \frac{k_{\mathrm{B2a}}^{k_{\mathrm{B2b}}}}{\left(k_{\mathrm{B2a}}^{k_{\mathrm{B2b}}} + \mathrm{PKA}^{k_{\mathrm{B2b}}}\right)}, \qquad (6-CB)$$

$$\frac{\mathrm{d}}{\mathrm{d}t}S_{\mathrm{PKA}} = k_{\mathrm{D1}} \times \mathrm{D} \times S_{\mathrm{OFF}} - k_{\mathrm{B2}} \times S_{\mathrm{PKA}} \times \frac{k_{\mathrm{D2a}}^{k_{\mathrm{D2b}}}}{\left(k_{\mathrm{D2a}}^{k_{\mathrm{D2b}}} + \mathrm{D}^{k_{\mathrm{D2b}}}\right)}, \qquad (6-SYN)$$

where k_{B1} is the rate constant of the transformation from S_{OFF} into S_{PKA}, which is brought about by the activity of the catalytic subunit of PKA or the protein D. However, the protein AD, through a Hill function with coefficient k_{D1b} and half saturation k_{D1a}, can inhibit this conversion. The recycling of S_{PKA} into S_{OFF} occurs with rate constant k_{B2}, but is inhibited by PKA and D through inhibiting Hill functions with coefficients k_{B2b} and k_{D2b}, respectively, and half saturations k_{B2a} and k_{D2a}, respectively. Also, activity of AD can convert S_{PKA} into S_{AD} with a rate constant k_{D3} and a Hill function with coefficient k_{D3b} and half saturation k_{D3a}.

The dynamics of the catalytic and regulatory subunits of PKA are adapted from a model presented by Pettigrew *et al.* (2005), where the changes to this model are described in the results. PKA dynamics are given in the following equations:

$$\frac{\mathrm{d}}{\mathrm{d}t}\mathrm{cAMP} = V_{\mathrm{m}} \times \frac{[5\mathrm{HT}]}{k_{5\mathrm{HT}} + [5\mathrm{HT}]} - (\mathrm{cAMP} - \mathrm{cAMP_{basal}}), \qquad (7)$$

$$\frac{\mathrm{d}}{\mathrm{d}t}R = K_{\mathrm{fpka}} \times \mathrm{RC} \times \mathrm{cAMP}^2 - K_{\mathrm{bpka}} \times \mathrm{R} \times \mathrm{C}, \qquad (8)$$

$$\frac{\mathrm{d}}{\mathrm{d}t}\mathrm{C} = K_{\mathrm{fpka}} \times \mathrm{RC} \times \mathrm{cAMP}^2 - K_{\mathrm{bpka}} \times \mathrm{R} \times \mathrm{C}, \qquad (9)$$

$$\frac{\mathrm{d}}{\mathrm{d}t}\mathrm{RC} = -K_{\mathrm{fpka}} \times \mathrm{RC} \times \mathrm{cAMP}^2 + K_{\mathrm{bpka}} \times \mathrm{R} \times \mathrm{C}, \qquad (10)$$

where V_{m} is the cAMP synthesis rate constant and $K_{5\mathrm{HT}}$ is the half saturation of the Hill function associated with cAMP synthesis. K_{fpka} is the rate constant associated with the dissociation of the catalytic and regulatory subunits, while the reassociation rate is given by K_{bpka}. The amount of PKA activity is set equal to the amount of the free catalytic subunit (C); PKA = C. The parameters associated with protein synthesis are given the subscript S to differentiate them from signaling complex dynamics. The synthesis of AD and D are given by the following equations:

$$\frac{\mathrm{d}}{\mathrm{d}t}\mathrm{AD} = k_{\mathrm{s1}} \times \frac{f(\mathrm{PKC},t)^{k_{\mathrm{s1b}}}}{k_{\mathrm{s1a}}^{k_{\mathrm{s1b}}} + f(\mathrm{PKC},t)^{k_{\mathrm{s1b}}}} - k_{s2} \times \mathrm{AD}, \qquad (11)$$

$$f(\mathrm{PKC},t) = \int_{t-\mathrm{intPKC}}^{t} \mathrm{PKC}(t) \times \mathrm{d}t, \qquad (12)$$

$$\frac{\mathrm{d}}{\mathrm{d}t}\mathrm{D} = k_{\mathrm{s3}} \times \frac{\mathrm{g}(\mathrm{PKA},t)^{k_{\mathrm{s3b}}}}{k_{\mathrm{s3a}}^{k_{\mathrm{s3b}}} + \mathrm{g}(\mathrm{PKA},t)^{k_{\mathrm{s3b}}}} - k_{s4} \times \mathrm{D}, \qquad (13)$$

$$\mathrm{g}(\mathrm{PKA},t) = \int_{t-\mathrm{intPKA}}^{t} \mathrm{PKA}(t - \text{delay D}) \times \mathrm{d}t, \qquad (14)$$

AD synthesis depends on the total activity of PKC Apl II over a previous time window of duration given by intPKC in Eqn (12).

© 2014 Federation of European Neuroscience Societies and John Wiley & Sons Ltd

The integration of PKC Apl II activity leads to the synthesis of AD through a Hill function with coefficient k_{S1b} and half saturation k_{S1a}. k_{S2} represents the AD degradation constant. Similarly, D synthesis depends on an integration of PKA activity over a time period of intPKA in Eqn (14), which leads to the synthesis of D with a rate constant of k_{S3} and through a Hill function with coefficient k_{S3b} and half saturation k_{S3a}. The degradation of D is given by rate constant k_{S4}. D leads to the transformation of S_{OFF} into S_{PKA}, which was described above in Eqn (6), while AD transforms S_{OFF} into S_{AD}, whose dynamics are modeled with the following equation:

$$\frac{d}{dt}S_{AD} = k_{C1} \times S_{OFF} \times AD - k_{A1} \times [5HT] \times S_{AD} + k_{A2} \times S_{ADON} - k_{C2} \times S_{AD} \times \frac{k_{C2a}^{k_{C2b}}}{k_{C2a}^{k_{C2b}} + AD^{k_{C2b}}}, \quad (15)$$

where k_{C1} is the rate constant associated with the transformation of S_{OFF} into S_{AD}, k_{C2} the rate constant of the recycling of S_{AD} into S_{OFF}, which can be inhibited by AD through a Hill function with coefficient k_{C2b} and half saturation k_{C2a}. Also, S_{AD} can become activated when 5HT transforms it into S_{ADON}, whose dynamics are given in the following equation:

$$\frac{d}{dt}S_{ADON} = k_{A1} \times [5HT] \times S_{AD} - k_{A2} \times S_{ADON}, \quad (16)$$

whose transformation and recycling rate constants are identical to those of S_{OFF} into S_{ON}. S_{ADON} activates PKC Apl II in an identical fashion to S_{ON} in Eqn (1).

The system was solved numerically by employing a 4th-order Runga–Kutta scheme to solve the differential equations and the Trapezoid Rule to solve the integrals (LeVeque, 2007). Parameter estimation was conducted with the help of the MATLAB Optimization Toolbox and Global Optimization Toolbox, specifically the functions lsqcurvefit, ga, and fmincon. These functions were used to minimize the least-squares distance between the modeling output and experimental data. Values of individual parameters are given in Table 1.

Results

PKC Apl II translocation desensitizes equally to spaced and continuous applications of 5HT when sensory neurons are co-cultured with motor neurons. *Aplysia* sensory neurons were microinjected with plasmid DNA encoding eGFP-PKC Apl II as described in methods. During spaced applications of 5HT, sensory neurons co-cultured with motor neurons were exposed to 5 × 5-min pulses of 10 μM 5HT with 15 min washes in between successive pulses. Translocation of eGFP-PKC Apl II was measured in the cell body and in the sensory neuron varicosities adjoining motor neuron processes in co-cultures. These varicosities have been shown to have a high probability of being synapses (Glanzman *et al.*, 1989a; Dale & Kandel, 1993; Hawver & Schacher, 1993; Conrad *et al.*, 1999). Indeed, *Aplysia* sensory neurons rapidly form glutamatergic synapses when cultured with their *in vivo* target motor neurons (Dale & Kandel, 1993; Conrad *et al.*, 1999) but not when cultured with a non-target motor neuron or with other sensory neurons (Glanzman *et al.*, 1989a; Hawver & Schacher, 1993). Prior to each experiment, synapse formation was measured for each sensory–motor neuron pair by assessing synaptic efficacy electrophysiologically to ensure that synapse formation had taken place. Following the first 5HT treatment, eGFP-PKC Apl II translocated from the cytosol to the plasma membrane (Fig. 1A). When 5HT was washed off, the protein reverted to the cytosol. When 5HT was added again, eGFP-PKC Apl II translocation desensitized, but to a much lesser extent than previously observed in the isolated cell body (Farah *et al.*, 2009) (Fig. 1B). After the fifth pulse of 5HT, PKC Apl II translocation normalized to 5 min was 0.61 ± 0.11 in the cell body and 0.53 ± 0.16 in the varicosities compared to 0.15 ± 0.05 in isolated sensory neurons (Fig. 1B and C; also Farah *et al.*, 2009). The amount of desensitization was similar in the cell body and the varicosities in spaced applications of 5HT [Fig. 1B and C; not significant in two-way ANOVA (location, time); $P > 0.05$]. Massed applications of 5HT were performed by continuously exposing co-cultured sensory and motor neurons to 10 μM 5HT for 85 min. Over time, eGFP-PKC Apl II translocation desensitized (Fig. 2A–C). By 25 min, PKC Apl II translocation normalized to 5 min was 0.45 ± 0.06 in the cell body and 0.49 ± 0.08 in the varicosities, and by 85 min translocation was 0.11 ± 0.04 in the cell body and -0.03 ± 0.08 in the varicosities. The amount of desensitization was similar in the cell body and the varicosities in massed applications of 5HT (Fig. 2B and C; no significant effect of location in ANOVA; $P > 0.05$), but greater than previously seen in isolated sensory neurons [0.28 ± 0.02 at the 85 min time point in isolated sensory neurons; Fig. 2B; (Farah *et al.*, 2009)].

Massed applications of 5HT resulted in a greater amount of desensitization of PKC translocation than spaced applications of 5HT when the final 85-min time points were used for comparison (translocation normalized to 5 min is 0.61 ± 0.11 in the cell body and 0.53 ± 0.16 in the varicosities for spaced 85-min and 0.11 ± 0.04 in the cell body and -0.03 ± 0.08 in the varicosities for massed 85-min). However, when comparison is made based on equivalent exposure times to 5HT there is no significant difference in the desensitization of eGFP-PKC Apl II (Fig. 3A and B; not significant in two-tailed Student's *t-test*). This observation suggests that when sensory neurons are paired with motor neurons, the desensitization of PKC Apl II is linear – it depends on the amount of time that the neuron is exposed to 5HT and not the pattern of exposure. These findings contrast to what was observed in isolated sensory neurons, where spaced applications of 5HT were found to cause an equivalent amount of desensitization when comparing between 85-min time points and much greater desensitization when comparing the massed 25-min time point to the spaced 85-min time point (Farah *et al.*, 2009).

PKA similarly mediates desensitization in both the cell body and the varicosities

We had previously shown that PKA activity increases desensitization of eGFP-PKC Apl II in isolated sensory neurons (Farah *et al.*, 2009). To determine whether PKA plays a similar role in sensory neurons co-cultured with motor neurons, a PKA inhibitor, KT5720, was applied during massed applications of 5HT, as described in Materials and Methods. KT5720 caused a decrease in the desensitization of eGFP-PKC Apl II translocation (Fig. 4A–D). A two-way ANOVA (drug, time) showed a significant effect of KT5720 ($P < 0.0001$) in both the cell body and the varicosities (Fig. 4E and F) implying that PKA increases desensitization, as was observed in isolated sensory neurons. The amount of inhibition by PKA was similar in the cell body and the varicosities (Fig. 4C and D; $P > 0.05$ for location in two-way ANOVA).

Protein translation only affected desensitization in varicosities

We have previously shown that applying a protein translation inhibitor to isolated sensory neurons causes an increase in desensitization

© 2014 Federation of European Neuroscience Societies and John Wiley & Sons Ltd

TABLE 1. Values of model parameters for both the cell body and synapse models

Parameter	Value		Notes	Found in equation(s)
	Cell body	Synapse		
k_{A2}	1	1	S_{ON} into S_{IN1}	2, 4
k_{S1a}	6	6	Half saturation of Hill function synthesizing AD	10
k_{D3b}	0.3372	0.3372	Hill coefficient of Hill function inhibiting S_{OFF} into S_{PKA} (via AD)	3, 6
k_{DAGp}	200	200	DAG synthesis rate constant	1
k_{DAGd}	10^2	10^2	DAG degradation rate constant	1
k_{A1}	10^5	10^5	S_{OFF} into S_{ON}	2,3
k_{S1b}	4	4	Hill coefficient of Hill function synthesizing AD	11
k_{S3}	0.4483	0.4483	D synthesis rate constant	13
k_{A3}	3	3	S_{IN1} to S_{OFF}	3, 4
k_{A4}	0.2371	0.2371	S_{IN1} to S_{IN2}	4, 5
k_{S3a}	6	6	Half saturation of Hill function synthesizing D	13
delayD	10	10	PKA delay in D synthesis	14
int*PKA*	15	15	PKA integration window	14
k_{D3}	0.0764	0.0764	S_{PKA} into S_{AD}	6, 15
k_{D3b}	0.1385	0.1385	Hill coefficient of Hill function activating S_{PKA} into S_{AD}	6, 15
k_{S1}	0.026	0.026	AD synthesis rate constant	11
k_{S2}	0.2	0.2	AD degradation rate constant	12
k_{C1}	2	2	S_{OFF} into S_{AD}	3, 15
k_{C2}	0.1	0.1	S_{AD} into S_{OFF}	3, 15
k_{S4}	0.2847	0.2847	D degradation rate constant	13
k_{D1}	8.0441	8.0441	S_{OFF} into S_{PKA} (via D)	3, 6
k_{D1a}	5.33×10^{-8}	5.33×10^{-8}	Half saturation of Hill function inhibiting S_{OFF} into S_{PKA} (via AD)	3, 6
V_m	3.6	3.6	cAMP synthesis rate constant	7
K_{fpka}	105	105	PKA subunit dissociation rate constant	8–10
int*PKC*	15	15	PKC integration window	12
k_{A5}	0.003	0.003	S_{IN2} to S_{OFF}	3, 5
k_{B2a}	0.5	0.5	Half saturation of Hill function inhibiting S_{PKA} into S_{OFF} (via PKA)	3, 6
k_{B2b}	6	6	Hill coefficient of Hill function inhibiting S_{PKA} into S_{OFF} (via PKA)	3, 6
k_{C2b}	1	1	Hill coefficient of Hill function inhibiting S_{AD} into S_{OFF}	3, 15
k_{B2}	0.2	0.2	S_{PKA} into S_{OFF}	3, 6
k_{D2b}	0.4187	0.4187	Hill coefficient of Hill function inhibiting S_{PKA} into S_{OFF} (via D)	3, 6
*K*5HT	14×10^{-6}	14×10^{-6}	Half saturation of Hill function synthesizing cAMP	7
K_{bpka}	3	3	PKA subunit reassociation rate constant	8–10
k_{B1}	0.1276	0.1276	S_{OFF} into S_{PKA} (via PKA)	3, 6
k_{D3a}	1.6×10^4	1.6×10^4	Half saturation of Hill function transforming S_{PKA} into S_{AD}	6, 15
k_{C2a}	1	1	Half saturation of Hill function inhibiting S_{AD} into S_{OFF}	3, 15
k_{B2a}	53.1	53.1	Half saturation of Hill function inhibiting S_{PKA} into S_{OFF} (via D)	3, 6
$cAMP_{basal}$	0.005	0.005	Basal concentration of cAMP	7
k_{S3b}	4	4	Hill coefficient of Hill function synthesizing D	13

during massed applications of 5HT (Farah *et al.*, 2009). To determine whether protein translation plays a similar role in sensory neurons co-cultured with motor neurons, a protein translation inhibitor, anisomycin, was applied during massed applications of 5HT. Anisomycin caused no significant change in the desensitization of eGFP-PKC Apl II translocation in the cell body of sensory neurons (Fig. 5A and E; no effect of anisomycin in two-way ANOVA, $P > 0.05$). However, anisomycin did cause a significant reduction in desensitization in varicosities (Fig. 5B and F; significant effect of anisomycin, $P < 0.0001$ in two-way ANOVA). Theses data represent the first difference in desensitization dynamics we observed between the cell body and the varicosities.

Interestingly, the amount of desensitization observed in varicosities with anisomycin is similar to the amount observed with the PKA inhibitor KT5720 (Fig. 5G; not significant in two-way ANOVA, $P > 0.05$). Also, anisomycin caused a decrease in desensitization in the varicosities during massed applications of 5HT whereas in isolated sensory neurons anisomycin had the opposite effect and actually increased desensitization (Farah *et al.*, 2009). This reversal of the effect of anisomycin on the desensitization of PKC Apl II translocation in the varicosities and its lack of effect in the cell body indicates that the signaling pathway responsible for PKC Apl II desensitization is significantly altered after synapse formation. We next used mathematical modeling in order to understand the changes being made to the signaling pathway responsible for the desensitization of PKC translocation after synapse formation.

Describing the model architecture

A model was previously created to explain this signaling network in isolated sensory neurons (Naqib *et al.*, 2011). Modifications were made to this model in order to explain the desensitization dynamics observed when the sensory neuron forms synapses with a motor neuron.

The basic unit of the model is the signaling complex, *S*, which consists of the 5HT GPCR and all of the downstream steps between the receptor and the production of DAG, which is capable of activating and translocating PKC Apl II to the membrane (Sossin, 2007; Sossin & Abrams, 2009). While this pathway consists of multiple steps, such as G-protein activation of phospholipase C and phospholipase D (Farah *et al.*, 2008), these are not likely to be important for modeling of desensitization, as in most systems the amount of the activatable GPCR is the rate-limiting quantity that is decreased during desensitization (Ferguson, 2001; Gainetdinov *et al.*, 2004; Hanyaloglu & von Zastrow, 2008), and throughout we will refer to *S* as the 5HT receptor, with the understanding that

© 2014 Federation of European Neuroscience Societies and John Wiley & Sons Ltd

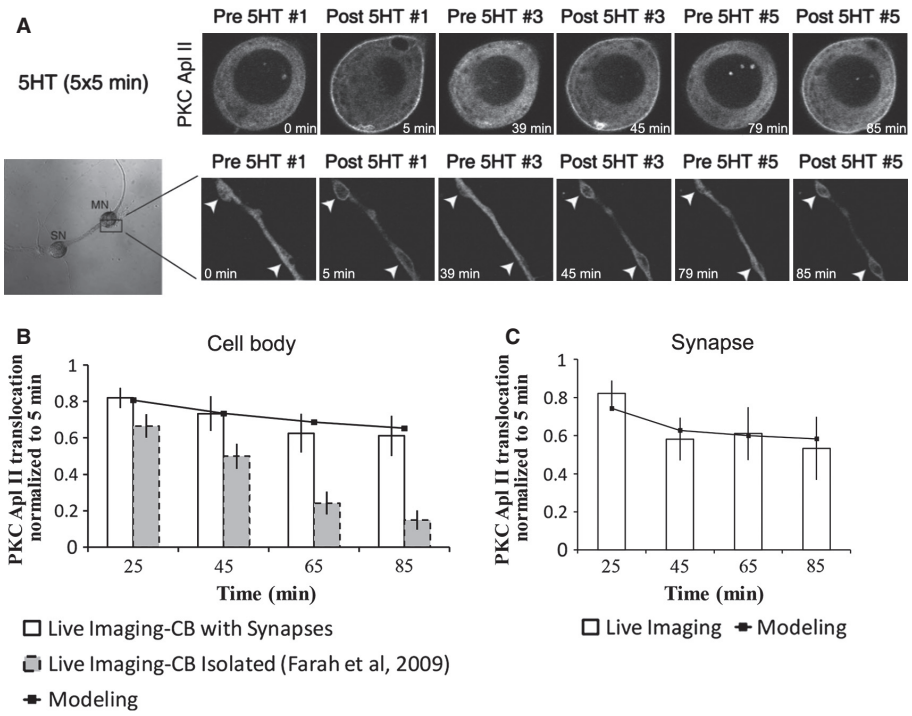

FIG. 1. PKC Apl II translocation in cell body and varicosities during spaced applications of 5HT. (A) Representative confocal fluorescence images of sensory neurons expressing eGFP-PKC Apl II during 5 × 5-min pulses of 5HT with 15-min washes. The top row illustrates PKC Apl II translocation in the cell body and the bottom row illustrates translocation in the varicosities. Quantification of PKC Apl II translocation (bars) and modeling output (line) in (B) the cell body (n = 3) and (C) the synapse (n = 13 varicosities in three neurons); CB, cell body.

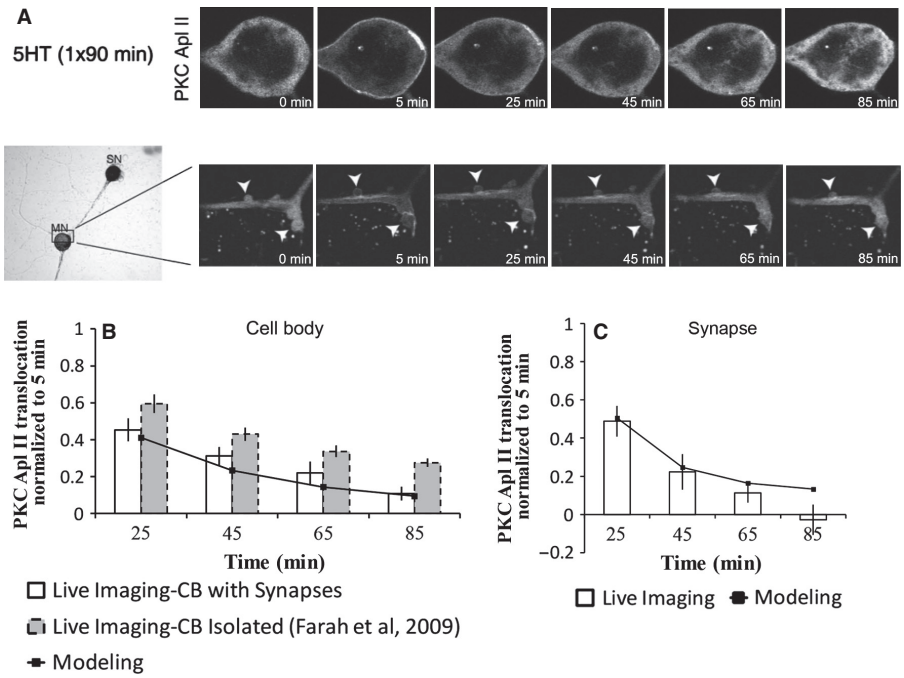

FIG. 2. PKC Apl II translocation in cell body and varicosity during massed applications of 5HT. (A) Representative confocal fluorescence images of sensory neurons expressing eGFP-PKC Apl II during an 85-min exposure to 5HT. The top row illustrates PKC Apl II translocation in the cell body and the bottom row illustrates translocation in the varicosities. (B and C) Quantification of PKC Apl II translocation (bars) and modeling output (line) in (B) cell bodies ($n \geq 4$) and (C) the synapse (n = 10 varicosities in five neurons); CB, cell body.

changes in S may also reflect changes in the signaling pathway between the 5HT receptor and PKC.

GPCRs can enter a number of different pathways, such that S can exist in several different states. We model the change in concentration of each state with respect to time. S can be in one of three types of state – an active state in which DAG is being produced and PKC is being translocated, an activatable state that is capable of being activated by 5HT and producing DAG and translocating PKC, or an

© 2014 Federation of European Neuroscience Societies and John Wiley & Sons Ltd

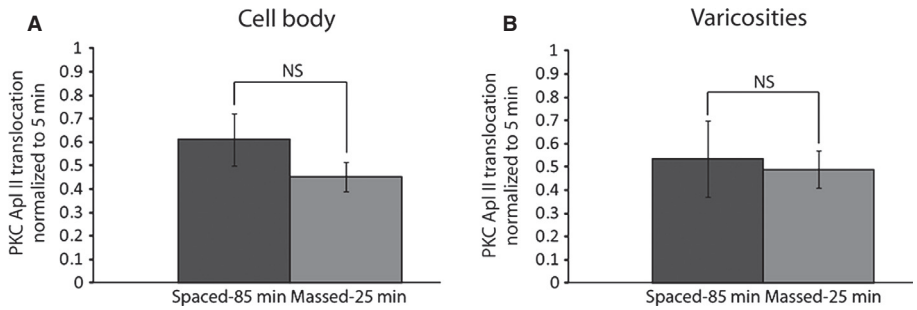

FIG. 3. Comparison of desensitization during spaced and massed applications of 5HT. Comparing the amount of desensitization of PKC Apl II translocation (data from Figs 1 and 2) after equivalent exposure times to 5HT (5 × 5-min 5HT pulses = 25 min massed 5HT) in (A) the cell body and (B) the varicosities. NS, not significant.

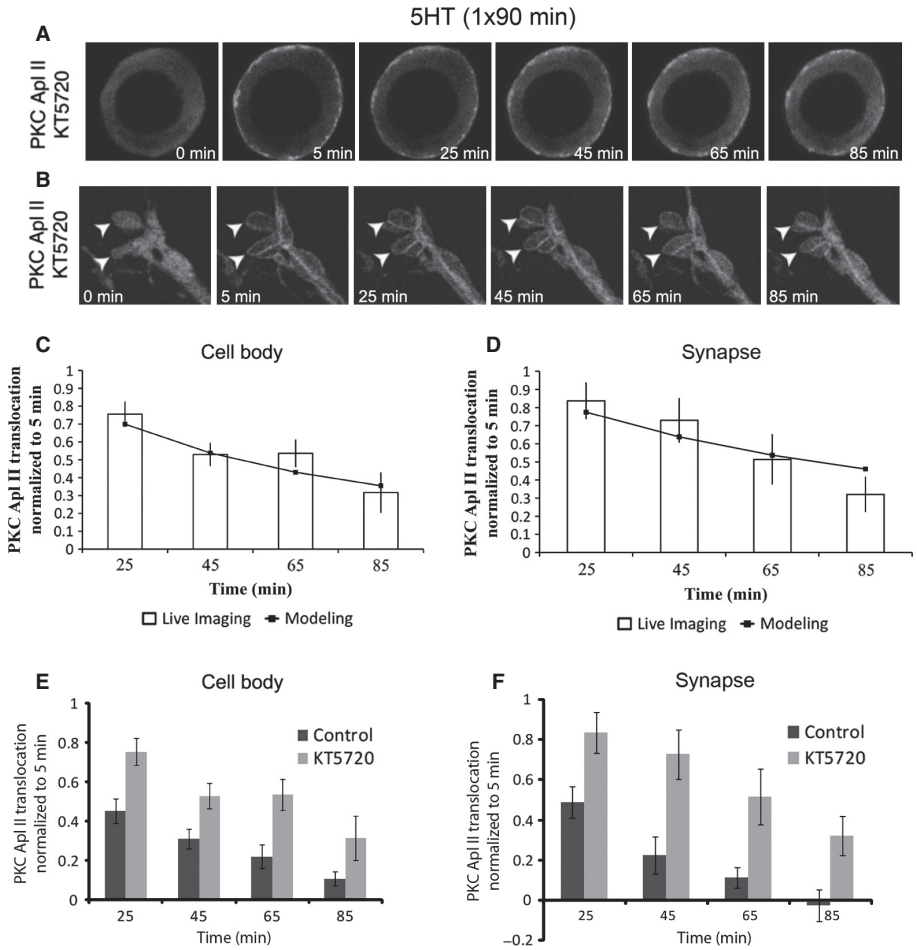

FIG. 4. PKC Apl II translocation in cell body and varicosity during massed applications of 5HT with KT5720. Representative confocal fluorescence images of (A) sensory neuron cell bodies and (B) varicosities expressing eGFP-PKC Apl II during an 85-min exposure to 5HT in the presence of the PKA inhibitor KT5720. (C and D) Quantification of PKC Apl II translocation (bars) and modeling output (line) in (C) cell bodies (n = 5) and (D) the synapse (n = 10 varicosities in five neurons). (E) Comparison of PKC Apl II translocation in the cell body of control (from Fig. 2B) vs. KT5720 treated cells. (F) Comparison of PKC Apl II translocation in the varicosities of control (from Fig. 2C) vs. KT5720-treated cells.

inactivated state in which 5HT will not cause PKC translocation. Thus, the ratio of S in activatable vs. inactivated will dictate the amount of translocation of PKC Apl II when 5HT is added, and thus the amount of desensitization.

The complete model architecture of the isolated sensory neuron model that has been previously examined and validated (Naqib *et al.*, 2011) is presented in Fig. 6A. The model components (color-coded) were developed sequentially, with maroon and black first then blue, red and finally green. The maroon component represents only the translocation of PKC to the plasma membrane and its subsequent dissociation from the membrane. The black component represents the homologous desensitization pathway that occurs even in the presence of a protein translation inhibitor and a PKA inhibitor. In this pathway, the S complex begins in S_{OFF}, which is then activated by 5HT to S_{ON}. The complex is then inactivated, S_{IN1}, from which it can then either quickly recover, returning to S_{OFF}, or be converted to a stably inactivated state S_{IN2}, from which it only recovers to S_{OFF} very slowly. When only this system is operative,

© 2014 Federation of European Neuroscience Societies and John Wiley & Sons Ltd

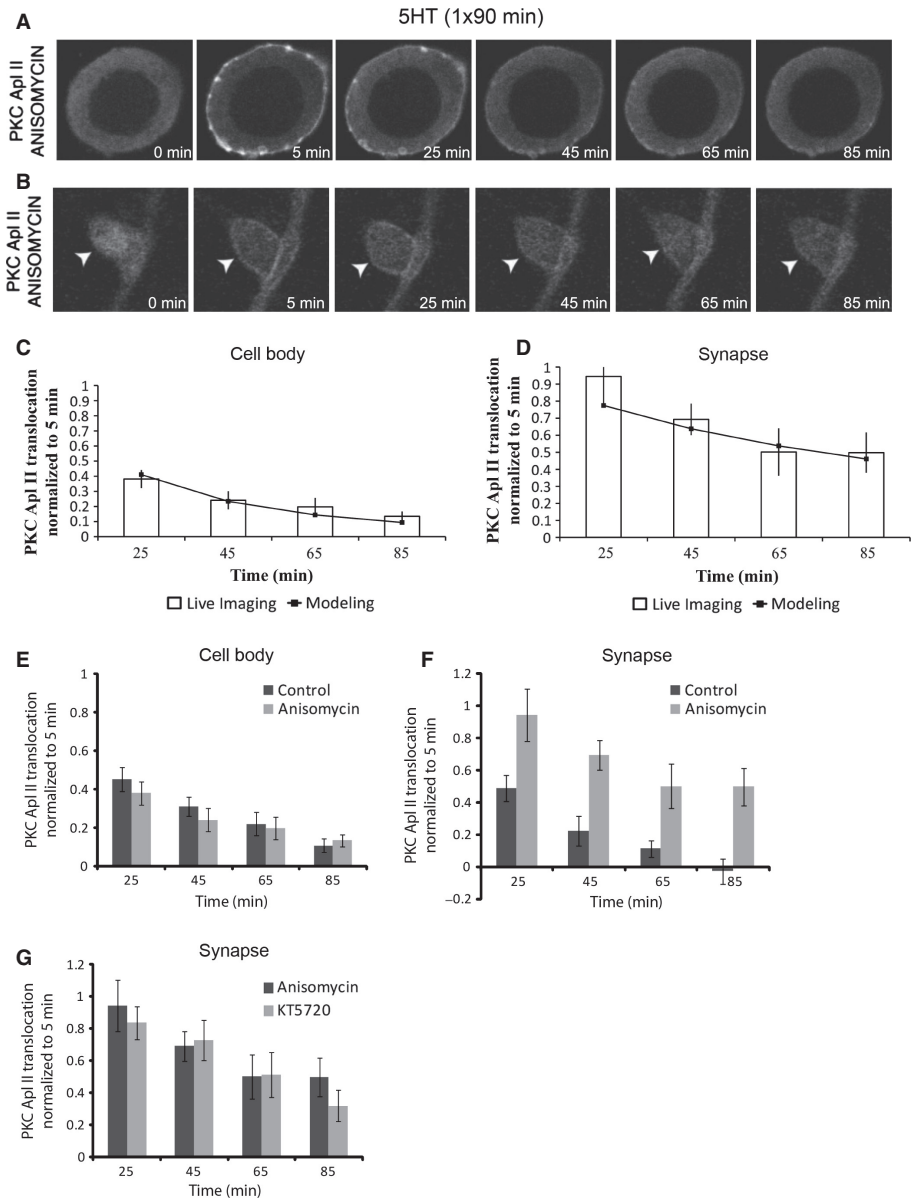

FIG. 5. PKC Apl II translocation in cell body and varicosity during massed applications of 5HT with anisomycin. Representative confocal fluorescence images of (A) sensory neuron cell bodies and (B) varicosities expressing eGFP-PKC Apl II during an 85-min exposure to 5HT in the presence of the protein translation inhibitor anisomycin. (C and D) Quantification of PKC Apl II translocation (bars) and modeling output (line) in (C) cell bodies ($n = 5$) and (D) the synapse ($n \geq 9$ varicosities in five neurons). (E) Comparison of PKC Apl II translocation in the cell body of control (from Fig. 2B) vs. anisomycin treated cells. (F) Comparison of PKC Apl II translocation in the varicosities of control (from Fig. 2C) vs. anisomycin-treated cells. (G) Comparison of PKC Apl II translocation in the varicosities of anisomycin-treated (Fig. 5D) vs. KT5720-treated (Fig. 4D) cells.

the S complex slowly accumulates in S_{IN2}. Both these components were required to fit the rate of desensitization that occurs in the absence of PKA and protein synthesis (Naqib *et al.*, 2011). The red component represents the additional pathways operative with no PKA activity but when protein synthesis is active. In this case, the hypothetical AD protein is produced and converts the S complex to S_{AD}, a state in which the receptor can be activated, $S_{AD(ON)}$, but not inactivated. The blue component represents the additional pathways operative with PKA activity but no protein synthesis. In this case, PKA activity converts the S_{OFF} complex to S_{PKA}, an inactivated state. The conversion of the S_{OFF} complex was necessitated by the ability of PKA to inactivate the complex even when 5HT was no longer present (Farah *et al.*, 2009). Interestingly, conversion from S_{PKA} to S_{OFF} occurs rapidly once PKA activity is removed, and thus the model predicts that recovery is faster when PKA activity is present and the S complex accumulates in S_{PKA} compared to when PKA activity is absent and the S complex accumulates in S_{IN2}. This prediction has been validated (Naqib *et al.*, 2011). The green component of the model represents the additional pathways operative when both PKA and protein synthesis are active. In this case, PKA induces protein synthesis of the hypothetical D protein that, similar to PKA, coverts S_{OFF} to S_{PKA}. To prevent D from overriding AD during massed applications of 5HT required AD to inhibit the actions of D (Naqib *et al.*, 2011), and these pathways are also outlined in green.

Two new models were created by modifying the isolated sensory neuron model. One model was created for the cell body (Fig. 6B) and one for the synapse (Fig. 6C). These changes were based on a

© 2014 Federation of European Neuroscience Societies and John Wiley & Sons Ltd

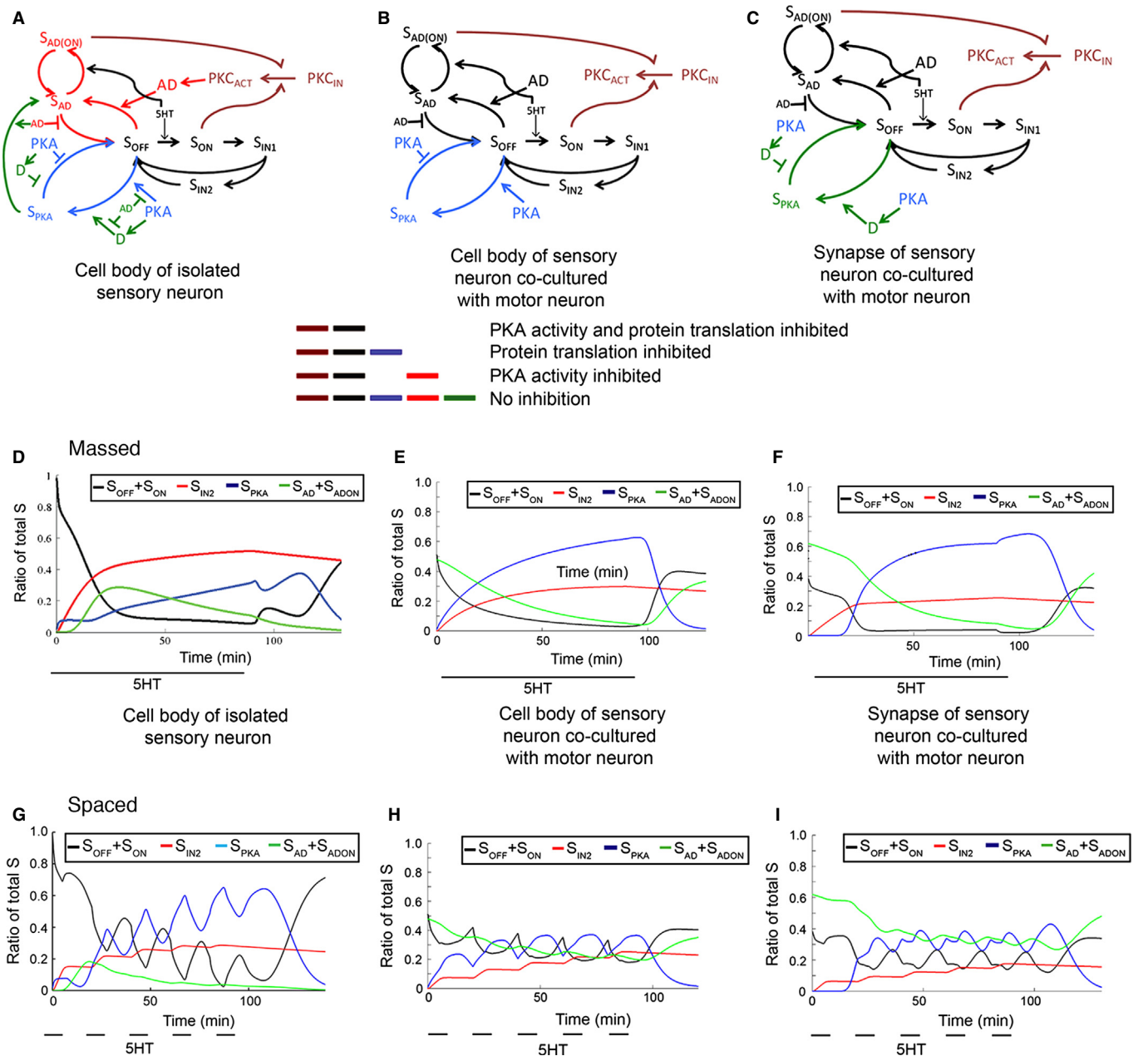

directed approach, testing models directly based on the findings of the new data as opposed to starting *de novo* and generating a new model. We were also guided by biological plausibility and known differences between signal transduction in the cell body and the synapse (see Discussion). The two new models share some common modifications from the isolated sensory neuron model. All of these shared modifications affected the dynamics of the protein AD, the hypothetical protein that prevents desensitization, and whose implementation was necessary for two reasons. First, as described above, applying a protein translation inhibitor during massed applications of 5HT no longer increased desensitization but in fact decreased it (Fig. 5). As the previous model accounted for protein synthesis-dependent protection from desensitization through the production of AD, this clearly needed to be modified. This finding suggests that rapid synthesis and degradation of AD was no longer occurring over the time course of these experiments and thus it appears that there should be a constant level of AD. AD is thus now part of the black component, present in the absence of PKA and protein synthesis. Second, spaced applications of 5HT no longer caused a significantly greater amount of desensitization than massed applications (Fig. 3). Previously, we explained this difference in desensitization due to stimulus patterns on the competition between AD and D (Naqib *et al.*, 2011). As this difference in desensitization is no longer occurring, it suggests removing the competition between AD and D. This uncoupling could be done by removing AD's inhibition of PKA and D's activity, and removing AD's ability to transform S_{PKA} into S_{AD}.

To determine whether these modifications were sufficient to fit the new data, we first fitted the new AD parameters to experiments in which a minimal part of the pathway was operative. Applying a PKA inhibitor reduces the model architecture to only the maroon and black components (Fig. 6). These components constitute the

© 2014 Federation of European Neuroscience Societies and John Wiley & Sons Ltd

FIG. 6. Model networks. The networks of the three models. In all models, *S* represents the signaling complex consisting of the 5HT receptor coupled to PKC activation and all other signaling components in between 5HT binding to the receptor and PKC activation (such as G-proteins and phospholipase C). (A) The original model (described in Naqib *et al.*, 2011) postulates that this complex can be in a number of different states that are either active (S_{ON} and $S_{AD(ON)}$), poised for activation (i.e. only 5HT is required to activate the receptor – S_{OFF} and S_{AD}) or inactivated (i.e. 5HT cannot activate the receptor – S_{IN1}, S_{IN2} and S_{PKA}). The difference between S_{IN1} and S_{IN2} is that while S_{IN1} is converted rapidly to S_{OFF}, S_{IN2} is only converted very slowly to S_{OFF}. S_{PKA} is an inactivated receptor state stimulated by PKA and the D (Desensitizer) protein acting on S_{OFF}. Active PKA and D protein inhibit the return of this receptor to the S_{OFF} state. S_{AD} is a receptor state that is induced by the AD (Anti-Desensitizer) protein acting on either S_{OFF} or S_{PKA}. The AD protein also inhibits PKA and the D protein from converting S_{OFF} to S_{PKA}. The signaling complex in this state can be activated by 5HT and the AD protein inhibits the return of this protein to the S_{OFF} state. The model also involves protein synthesis of the AD protein downstream of PKC activity and protein synthesis of the D protein downstream of PKA acti vity. The colors correspond to the components of the models (see diagram). The models were constructed in a sequential manner (Naqib *et al.*, 2011). First, the components outlined in black and maroon were fitted to data generated in the absence of protein synthesis and PKA. The maroon component describes the translocation of PKC to the membrane and its subsequent dissociation from the membrane. The black module represents the homologous desensitization pathway. Following completion of these components, the component outlined in blue was constructed with data generated in the absence of protein synthesis but the presence of PKA, and represents the PKA-mediated desensitization pathway. The red component was constructed with data generated in the presence of protein synthesis but the absence of PKA, and represents the AD pathway induced by production of the AD protein. Finally, the green component was constructed in the presence of both PKA and protein synthesis, and represents both the desensitization pathway induced by synthesis of the D protein and the interactions between the AD and D pathway. (B) The model network of PKC translocation in the cell body of co-cultured sensory–motor neurons. AD is now a constant and thus the AD pathway is represented in black. There is no protein synthesis of D and thus the green components have also been removed. (C) The model network of PKC translocation at the synapse of co-cultured sensory–motor neurons. As in (B), AD is a constant so the AD pathway is represented in black. PKA acts only through synthesis of D in this model and thus the blue pathways (PKA and no protein synthesis) are now green (no inhibition). (D–F) Distribution of the signaling complexes during massed applications of 5HT either with (D) the old model described in Naqib *et al.*, 2011 or the new models at (E) the cell body and (F) the synapse of a sensory neuron, co-cultured with a motor neuron. (E and F) Modeling of *S* dynamics in response to experimental protocol from Fig. 2A. The black line represents the ratio of S_{OFF} and S_{ON} to total *S*, the red line the ratio of S_{IN2} to total *S*, the blue line the ratio of S_{PKA} to total *S*, and the green line represents the ratio of S_{AD} and S_{ADON} to total *S*. (G–I) Distribution of the signaling complexes during spaced applications of 5HT either (G) with the old model described in Naqib *et al.*, 2011 or the new models at (H) the cell body and (I) the synapse of a sensory neuron co-cultured with a motor neuron. H and I represent modeling of *S* dynamics in response to the experimental protocol from Fig. 1A.

homologous desensitization pathway and the AD protection from desensitization pathway. A constant value of AD was estimated by fitting the model to eGFP-PKC Apl II translocation measurements taken during a continuous 90-min application of 5HT in the presence of the PKA inhibitor KT5720 (Fig. 4C and D). The parameter estimation methods used are outlined in Materials and Methods. A suitable fit to the data was achieved by setting the constant concentration of AD at 0.0447 (arbitrary units) in the cell body and 0.0754 (arbitrary units) in the synapse. Constant AD improved the least-squares fit for the cell body data from 0.026 to 0.015 and at the synapse from 0.056 to 0.032 (see fit of the model to the data in Fig. 4C and D).

The cell body-specific modifications only involved removing D activity. Applying a protein translation inhibitor during massed training did not cause a significant change in the desensitization of PKC translocation. This finding suggests that D is not active in the cell body. In addition to the modifications to AD described above, removing D was able to suitably fit the PKC Apl II translocation dynamics at the cell body without further changes (Fig. 5C; least-squares fit improved from 0.41 to 0.080 after removing D). In contrast, at the synapse, applying a protein translation inhibitor decreased desensitization significantly. This finding suggests that D is generated by protein synthesis at the synapse. Interestingly, although applying a PKA inhibitor during massed application of 5HT caused a significant decrease in desensitization, it did not cause a significantly different amount of desensitization compared to when a protein translation inhibitor was applied (Fig. 5G). This observation suggests that PKA's effects are mediated through D alone and not directly. Thus, PKA's ability to transform S_{OFF} into S_{PKA} was removed at the synapse. This modification resulted in a suitable fit to the data at the synapse in the absence of protein synthesis (Fig. 5D; the least-squares fit improved from 0.41 to 0.0054).

Applying 5HT with no inhibitory drugs results in similar amounts of desensitization at the cell body and synapse during both spaced and massed applications of 5HT (Fig. 3). However, at the cell body the amount of desensitization with no drugs and with anisomycin are similar (Fig. 5E). Thus, the model consisting of a homologous desensitization pathway, a PKA-dependent desensitization pathway, and an AD protection from desensitization pathway with a constant amount of AD is sufficient to explain the signaling network mediating the desensitization of PKC translocation at the cell body [spaced, least-squares value of 0.0057 compared to fit of 0.49 with the old model (Fig. 1B); massed, least-squares value of 0.014 compared to 0.092 with the old model (Fig. 2B)].

The desensitization of PKC translocation at the synapse required the synthesis and activity of D. D is necessary as applying protein translation inhibitor significantly reduced desensitization (Fig. 5F), meaning that removing the inhibitor would allow D to become active and increase desensitization. Several parameters are involved in D synthesis, degradation and activity (Table 1). Only one needed to be altered from the original isolated sensory neuron model – the threshold of the Hill function regulating D synthesis (k_{S3a}). Using a parameter estimation method it was found that a value of 17.9512 (originally 6 in the isolated sensory neuron model) resulted in a suitable fit to both spaced and massed applications of 5HT (least-squares value for spaced improved from 0.84 to 0.015 while the least-squares fit for massed was actually increased from 0.032 to 0.051 by this modification; Figs 1 and 2).

To examine the differences made to the model we plotted the distribution of the signaling complexes during massed (Fig. 6D–F) and spaced (Fig. 6G–I) applications of 5HT either with the old model or the new models at the cell body and the synapse. A major difference during massed application is the increased desensitization (sum of S_{PKA} and S_{IN2}) due to the lack of an increase in S_{AD} because AD is no longer being synthesized. This is exacerbated by an increase in the amount of *S* present in S_{PKA} due to the lack of AD inhibition of the S_{off}-to-S_{PKA} pathway. Without inhibitors, the cell body and synapse appear similar but the conversion of S_{off} to S_{PKA} is protein synthesis-dependent at the synapse but not in the cell body. This can be seen by the delay in S_{PKA} in Fig. 6F compared to Fig. 6E. The decreased desensitization in spaced applications of 5HT (mainly mediated by a decreased build-up of receptor in S_{PKA}) is mostly mediated by the increased level of receptor in S_{AD}, due to the constant AD in the new model as opposed to the

© 2014 Federation of European Neuroscience Societies and John Wiley & Sons Ltd

old model, where AD synthesis was minimal during spaced training.

Discussion

We previously studied the desensitization of PKC translocation in response to different patterns of 5HT application in isolated *Aplysia* sensory neurons. In that study we found that spaced applications of 5HT caused greater desensitization than massed applications of 5HT. In the present study, we expanded our work by examining the desensitization of PKC translocation in co-cultured sensory and motor neurons, where the sensory neuron has formed synaptic connections with the motor neuron. We found that synapse formation results in a change in the desensitization of PKC translocation, spaced applications of 5HT no longer causing greater desensitization than massed applications. This suggests that the sensory neuron has undergone a change during synapse formation in the signaling network regulating the translocation and activation of PKC. Furthermore, we also found differences in the role of protein synthesis between isolated and co-cultured sensory neurons. In isolated sensory neurons, applying a protein translation inhibitor had a differential effect on spaced and massed applications of 5HT, reducing desensitization during spaced applications of 5HT and increasing desensitization during massed applications of 5HT (Farah *et al.*, 2009). We found that applying a protein translation inhibitor to sensory neurons co-cultured with motor neurons only reduces desensitization in the varicosities. Applying a PKA inhibitor was found to decrease desensitization in both the cell body and varicosities of co-cultured sensory neurons, similar to isolated sensory neurons (Farah *et al.*, 2009).

In order to explain these differences we modified our original isolated sensory neuron model of the signaling network underlying the desensitization of PKC translocation (Naqib *et al.*, 2011). We created two new models – one of the cell body of sensory neurons co-cultured with motor neurons and one of the synapses of these sensory neurons. These new models were able to explain the change in desensitization of PKC translocation by assuming changes in protein expression and location after synapse formation. The models were able to explain the reduction in desensitization following spaced applications of 5HT by reducing PKA's ability to increase desensitization. In the original model, PKA could directly and indirectly, through D activity, increase desensitization. In the sensory–motor neuron pair models, PKA could only directly increase desensitization in the cell body and acted exclusively through D in the synapse. The increase in desensitization following massed desensitization was modeled by reducing AD's ability to protect *S* from inactivation.

We do not argue that these models are unique in being able to explain the new desensitization dynamics. We have not verified these models with additional experiments and it is possible that other network architectures or parameter values could model these experimental findings. However, we developed these models from the original isolated sensory neuron model, which was experimentally validated, with the principle of least modifications necessary to explain the new data. Requiring the smallest number of modifications to the signaling network in order to elicit new behavior is more biologically plausible than reconstructing the network from the ground up. Furthermore, as discussed below, these modifications are biologically plausible. Our original model proposed a biochemical method of differentiating between spaced and massed stimuli. These new models provide an example of how a cell can restructure a biochemical signaling network in order to modulate its response to the same 5HT stimulus.

Synapse formation causes a change and redistribution of protein expression and activity

The cell body and synapse models share some common modifications. In both models, the concentration of the protein AD, which decreases desensitization, was held at a fixed amount whereas in the isolated sensory neuron model, AD synthesis was dependent on PKC activity. This modification accounted for the observation that applying a protein translation inhibitor could no longer increase desensitization as it did in isolated sensory neurons. We were unable to remove AD completely from the model as that caused too great a desensitization. Furthermore, spaced and massed applications of 5HT no longer caused a differential desensitization of PKC translocation. In the isolated sensory neuron model, competition between AD and D carried out this differential desensitization. As spaced and massed applications of 5HT no longer caused a differential desensitization of PKC translocation, much of this competition was uncoupled in both models, leaving AD and D to interact with just S_{OFF} and not each other.

In the isolated sensory neuron AD's function was to prevent *S* inactivation and desensitization of PKC translocation. AD was hypothesized to bind the GPCR in either the S_{OFF} or S_{PKA} state. This binding was hypothesized to either retain the GPCR on the membrane or cause its recycling back to the membrane. The new models retain AD's ability to prevent inactivation of the GPCR; however, the new AD does not affect S_{PKA}. These modifications suggest that following synapse formation the original isolated sensory neuron AD protein is replaced with a protein capable of capturing the GPCR in the same S_{AD} state but lacking some of the original capabilities of AD.

AD was hypothesized to be a PDZ protein (Naqib *et al.*, 2011); these are adapter proteins capable of retaining GPCRs on the membrane (Romero *et al.*, 2011). Many PDZ proteins have been identified with functions varying from tethering the GPCR to the plasma membrane to directing the assembly of accessory proteins to affecting GPCR trafficking (Jean-Alphonse & Hanyaloglu, 2011; Romero *et al.*, 2011). The AD of the new models shares some of these functionalities, making it also likely to be a PDZ protein. It is plausible that there are multiple PDZ proteins capable of binding the GPCR responsible for activating PKC, and that they are differentially expressed in the isolated sensory neuron and sensory neuron co-cultured with a motor neuron, suggesting that synapse formation causes a switch in expression of PDZ proteins.

Another alteration to protein expression involved both PKA and the hypothetical protein D. Inhibiting protein translation only reduced desensitization in the synapse and had no effect on the cell body, suggesting that D activity was only present in the synapse. Furthermore, applying a PKA inhibitor resulted in a decrease in desensitization equivalent to the decrease seen after inhibition of protein translation. This observation suggests that PKA was not directly causing desensitization in the synapse but was acting only through D activity. Our model suggests that following synapse formation the expression and activity of D is redistributed from the cell body and to the synapse. Redistribution of protein expression following synapse formation has been previously observed. For example, mRNA of syntaxin, a protein involved in vesicle docking and fusion during neurotransmitter release, is initially concentrated at the axon hillock but then becomes targeted away after synapse formation (Hu *et al.*, 2003). Another example is sensorin, whose mRNA decreases in concentration at the axon hillock and gets targeted to distal sites after synapse formation (Hu *et al.*, 2002).

© 2014 Federation of European Neuroscience Societies and John Wiley & Sons Ltd

Our model hypothesizes that, at the synapse, PKA does not drive the receptor to S_{PKA}; only D has this ability. The differential activity of PKA can also be explained by a differential distribution of PKA subtypes between the cell body and synapse. PKA is composed of catalytic subunits inhibited by bound regulatory (R) subunits (Corbin *et al.*, 1973; Corbin & Keely, 1977; Potter & Taylor, 1979). There are two known classes of R subunits – RI and RII (Reimann *et al.*, 1971; Corbin *et al.*, 1975). In *Aplysia*, RI is expressed in the cell body of sensory neurons while RII is located in synapses (Liu *et al.*, 2004). Not only are these subtypes differentially expressed in the cell body and synapse but they also have unique preferences to cellular structures and locations. Aside from inhibiting the catalytic subunit of PKA, the R subunit is also responsible for binding to A-kinase-anchoring proteins (AKAPs), a large family that targets PKA to specific subcellular compartments and assembles multi-protein signal complexes in order to facilitate signal propagation through specific pathways (Pidoux & Tasken, 2010). The RI and RII subunits have unique populations of AKAPs to which they bind, as well as a small subset of AKAPs that are common to the two subunits (Huang *et al.*, 1997; Angelo & Rubin, 1998; Li *et al.*, 2001). In turn, different AKAPs also have unique subcellular targets and molecular binding partners (Wong & Scott, 2004). Thus, with the cell body and synapse expressing different PKA regulatory subunits, it is possible that different signaling pathways are being activated by PKA in each compartment. The RI subunit might directly affect S_{OFF} and not D synthesis while the RII subunit would only affect PKC translocation through D activity.

Comparison of findings from cultured cells and ganglia

Our investigations have been limited to *Aplysia* sensory and motor neurons cultured in dishes. Desensitization of PKC Apl II activation has been observed in intact ganglia where a second application of 5HT was found to facilitate depressed synapses, a process mediated by PKC Apl II (Manseau *et al.*, 2001), half as much as the first application (Dumitriu *et al.*, 2006). There may also be differences in the state of the 5HT receptor coupled to PKC in the ganglia, as opposed to in culture, as the 5HT antagonist spiperone, which is capable of blocking PLC-coupled 5HT receptors in mammals (Hoyer *et al.*, 1994), blocks PKC-mediated downstream effects of 5HT in ganglia (Dumitriu *et al.*, 2006) but not in cultured neurons (Nagakura *et al.*, 2010). One explanation is that the 5HT receptor responsible for activating PKC Apl II is modified by receptor-binding proteins. These modifications could affect its antagonist specificity as well as its internalization and trafficking, causing differential desensitization dynamics and drug interactions. Our results suggest that there is a great deal of complexity in the regulation of G-protein signaling and distinct regulation of these GPCRs may explain differences, not only between cultured neurons and neurons in the animal but also during development, ageing and responses to external agents such as stress.

Acknowledgements

This study was supported by Canadian Institutes of Health Research (CIHR) Grant MOP 12046. W.S.S. is a James McGill Professor. Authors declare no conflict of interest.

Abbreviations

5HT, serotonin; AD, Anti-Desensitizer; CB, cell body (model); D, Desensitizer; DAG, diacylglycerol; eGFP, enhanced green-fluorescent protein; GPCR, G-protein-coupled receptor; PKA, protein kinase A; PKC, protein kinase C; S, signaling complex; SYN, synapse (model).

References

Angelo, R. & Rubin, C.S. (1998) Molecular characterization of an anchor protein (AKAPCE) that binds the RI subunit (RCE) of type I protein kinase A from *Caenorhabditis elegans*. *J. Biol. Chem.*, **273**, 14633–14643.

Brunelli, M., Castellucci, V. & Kandel, E.R. (1976) Synaptic facilitation and behavioral sensitization in *Aplysia*: possible role of serotonin and cyclic AMP. *Science*, **194**, 1178–1181.

Casadio, A., Martin, K.C., Giustetto, M., Zhu, H., Chen, M., Bartsch, D., Bailey, C.H. & Kandel, E.R. (1999) A transient, neuron-wide form of CREB-mediated long-term facilitation can be stabilized at specific synapses by local protein synthesis. *Cell*, **99**, 221–237.

Castellucci, V. & Kandel, E.R. (1976) Presynaptic facilitation as a mechanism for behavioral sensitization in *Aplysia*. *Science*, **194**, 1176–1178.

Conrad, P., Wu, F. & Schacher, S. (1999) Changes in functional glutamate receptors on a postsynaptic neuron accompany formation and maturation of an identified synapse. *J. Neurobiol.*, **39**, 237–248.

Corbin, J. & Keely, S. (1977) Characterization and regulation of heart adenosine 3′:5′-monophosphate-dependent protein kinase isozymes. *J. Biol. Chem.*, **252**, 910–918.

Corbin, J., Soderling, T. & Park, C. (1973) Regulation of adenosine 30,50-monophosphate-dependent protein kinase. I. Preliminary characterization of the adipose tissue enzyme in crude extracts. *J. Biol. Chem.*, **248**, 1813–1821.

Corbin, J., Keely, S. & Park, C. (1975) The distribution and dissociation of cyclic adenosine 3′:5′-monophosphate-dependent protein kinases in adipose, cardiac, and other tissues. *J. Biol. Chem.*, **250**, 218–225.

Dale, N. & Kandel, E.R. (1993) L-glutamate may be the fast excitatory transmitter of *Aplysia* sensory neurons. *Proc. Natl. Acad. Sci. USA*, **90**, 7163–7167.

Dumitriu, B., Cohen, J., Wan, Q., Negroiu, A. & Abrams, T.W. (2006) Serotonin receptor antagonists discriminate between PKA- and PKC-mediated plasticity in *Aplysia* sensory neurons. *J. Neurophysiol.*, **95**, 2713–2720.

Dunn, T.W., Farah, C.A. & Sossin, W.S. (2012) Inhibitory responses in *Aplysia* pleural sensory neurons act to block excitability, transmitter release, and PKC Apl II activation. *J. Neurophysiol.*, **107**, 292–305.

Farah, C.A. & Sossin, W.S. (2011a) Live-imaging of PKC translocation in Sf9 cells and in *Aplysia* sensory neurons. *J. Vis. Exp.*, **50**, 2516.

Farah, C.A. & Sossin, W.S. (2011b) A new mechanism of action of a C2 domain-derived novel PKC inhibitor peptide. *Neurosci. Lett.*, **504**, 306–310.

Farah, C., Nagakura, I., Weatherill, D., Fan, X. & Sossin, W.S. (2008) Physiological role for phosphatidic acid in the translocation of the novel protein kinase C Apl II in *Aplysia* neurons. *Mol. Cell. Biol.*, **28**, 4719–4733.

Farah, C., Weatherill, D., Dunn, T.W. & Sossin, W.S. (2009) PKC differentially translocates during spaced and massed training in *Aplysia*. *J. Neurosci.*, **29**, 10281–10286.

Farah, C.A., Lindeman, A.A., Siu, V., Gupta, M.D. & Sossin, W.S. (2012) Autophosphorylation of the C2 domain inhibits translocation of the novel protein kinase C (nPKC) Apl II. *J. Neurochem.*, **123**, 360–372.

Ferguson, S.S. (2001) Evolving concepts in G protein-coupled receptor endocytosis: the role in receptor desensitization and signaling. *Pharmacol. Rev.*, **53**, 1–24.

Gainetdinov, R.R., Premont, R.T., Bohn, L.M., Lefkowitz, R.J. & Caron, M.G. (2004) Desensitization of G protein-coupled receptors and neuronal functions. *Annu. Rev. Neurosci.*, **27**, 107–144.

Glanzman, D.L., Kandel, E.R. & Schacher, S. (1989a) Identified target motor neuron regulates neurite outgrowth and synapse formation of *Aplysia* sensory neurons in vitro. *Neuron*, **3**, 441–450.

Glanzman, D.L., Mackey, S.L., Hawkins, R.D., Dyke, A.M., Lloyd, P.E. & Kandel, E.R. (1989b) Depletion of serotonin in the nervous system of *Aplysia* reduces the behavioral enhancement of gill withdrawal as well as the heterosynaptic facilitation produced by tail shock. *J. Neurosci.*, **9**, 4200–4213.

Hanyaloglu, A.C. & von Zastrow, M. (2008) Regulation of GPCRs by endocytic membrane trafficking and its potential implications. *Annu. Rev. Pharmacol.*, **48**, 537–568.

Hawver, D.B. & Schacher, S. (1993) Selective fasciculation as a mechanism for the formation of specific chemical connections between *Aplysia* neurons in vitro. *J. Neurobiol.*, **24**, 368–383.

Hoyer, D., Clarke, D., Fozard, J., Hartig, P., Martin, G., Mylecharane, E., Saxena, P. & Humphrey, P. (1994) International Union of Pharmacology classification of receptors for 5-hydroxytryptamine (serotonin). *Pharmacol. Rev.*, **46**, 157–203.

© 2014 Federation of European Neuroscience Societies and John Wiley & Sons Ltd

Hu, J., Meng, X. & Schacher, S. (2002) Target Interaction regulates distribution and stability of specific mRNAs. *J. Neurosci.*, **22**, 2669–2678.

Hu, J., Meng, X. & Schacher, S. (2003) Redistribution of syntaxin mRNA in neuronal cell bodies regulates protein expression and transport during synapse formation and long-term synaptic plasticity. *J. Neurosci.*, **23**, 1804–1815.

Hu, J.Y., Goldman, J., Wu, F. & Schacher, S. (2004) Target-dependent release of a presynaptic neuropeptide regulates the formation and maturation of specific synapses in *Aplysia*. *J. Neurosci.*, **24**, 9933–9943.

Hu, J.Y., Wu, F. & Schacher, S. (2006) Two signaling pathways regulate the expression and secretion of a neuropeptide required for long-term facilitation in *Aplysia*. *J. Neurosci.*, **26**, 1026–1035.

Huang, L.J., Durick, K., Weiner, J.A., Chun, J. & Taylor, S.S. (1997) D-AKAP2, a novel protein kinase A anchoring protein with a putative RGS domain. *Proc. Natl. Acad. Sci. USA*, **94**, 11184–11189.

Jean-Alphonse, F. & Hanyaloglu, A.C. (2011) Regulation of GPCR signal networks via membrane trafficking. *Mol. Cell. Endocrinol.*, **331**, 205–214.

Jin, I., Kandel, E.R. & Hawkins, R.D. (2011) Whereas short-term facilitation is presynaptic, intermediate-term facilitation involves both presynaptic and postsynaptic protein kinases and protein synthesis. *Learn. Memory*, **18**, 96–102.

Kandel, E. (2001) The molecular biology of memory storage: a dialogue between genes and synapses. *Science*, **294**, 1030–1038.

Lee, Y., Choi, S., Lee, S., Kim, H. & Park, H. (2009) Identification of a serotonin receptor coupled to adenylyl cyclase involved in learning-related heterosynaptic facilitation in *Aplysia*. *Proc. Natl. Acad. Sci. USA*, **106**, 14634–14639.

LeVeque, R.J. (2007) *Finite Difference Methods for Ordinary and Partial Differential Equations*. Society for Industrial and Applied Mathematics, Philadelphia, PA.

Li, H., Degenhardt, B., Tobin, D., Yao, Z.X., Tasken, K. & Papadopoulos, V. (2001) Identification, localization, and function in steroidogenesis of PAP7: a peripheral-type benzodiazepine receptor and PKA (RIalpha)-associated protein. *Mol. Endocrinol.*, **15**, 2211–2228.

Liu, J., Hu, J., Schacher, S. & Schwartz, J. (2004) The two regulatory subunits of *Aplysia* cAMP-dependent protein kinase mediate distinct functions in producing synaptic plasticity. *J. Neurosci.*, **24**, 2465–2474.

Manseau, F., Fan, X., Hueftlein, T., Sossin, W. & Castellucci, V. (2001) Ca^{2+}-independent protein kinase C Apl II mediates the serotonin-induced facilitation at depressed *Aplysia* sensorimotor synapses. *J. Neurosci.*, **21**, 1247–1256.

Marinesco, S., Wickremasinghe, N., Kolkman, K.E. & Carew, T.J. (2004) Serotonergic modulation in *Aplysia*. II. Cellular and behavioral consequences of increased serotonergic tone. *J. Neurophysiol.*, **92**, 2487–2496.

Martin, K.C. (2004) Local protein synthesis during axon guidance and synaptic plasticity. *Curr. Opin. Neurobiol.*, **14**, 305–310.

Martin, K.C., Casadio, A., Zhu, H., Yaping, E., Rose, J.C., Chen, M., Bailey, C.H. & Kandel, E.R. (1997) Synapse-specific, long-term facilitation of *Aplysia* sensory to motor synapses: a function for local protein synthesis in memory storage. *Cell*, **91**, 927–938.

Nagakura, I., Dunn, T., Farah, C., Heppner, A., Li, F. & Sossin, W. (2010) Regulation of protein kinase C Apl II by serotonin receptors in *Aplysia*. *J. Neurochem.*, **115**, 994–1006.

Naqib, F., Farah, C.A., Pack, C.C. & Sossin, W.S. (2011) The rates of protein synthesis and degradation account for the differential response of neurons to spaced and massed training protocols. *PLoS Comput. Biol.*, **7**, e1002324.

Naqib, F., Sossin, W.S. & Farah, C.A. (2012) Molecular determinants of the spacing effect. *Neural Plast.*, **2012**, 581291.

Pettigrew, D.B., Smolen, P., Baxter, D.A. & Byrne, J.H. (2005) Dynamic properties of regulatory motifs associated with induction of three temporal domains of memory in *Aplysia*. *J. Comput. Neurosci.*, **18**, 163–181.

Pidoux, G. & Tasken, K. (2010) Specificity and spatial dynamics of protein kinase A signaling organized by A-kinase-anchoring proteins. *J. Mol. Endocrinol.*, **44**, 271–284.

Potter, R. & Taylor, S. (1979) Relationships between structural domains and function in the regulatory subunit of cAMP-dependent protein kinases I and II from porcine skeletal muscle. *J. Biol. Chem.*, **254**, 2413–2418.

Reimann, E., Waslh, D. & Krebs, E. (1971) Purification and properties of rabbit skeletal muscle adenosine 3′,5′-mono- phosphate-dependent protein kinases. *J. Biol. Chem.*, **246**, 1986–1995.

Romero, G., von Zastrow, M. & Friedman, P.A. (2011) Role of PDZ proteins in regulating trafficking, signaling, and function of GPCRs: means, motif, and opportunity. *Adv. Pharmacol.*, **62**, 279–314.

Schacher, S., Wu, F., Panyko, J.D., Sun, Z.Y. & Wang, D. (1999) Expression and branch-specific export of mRNA are regulated by synapse formation and interaction with specific postsynaptic targets. *J. Neurosci.*, **19**, 6338–6347.

Sossin, W. (2007) Isoform specificity of protein kinase Cs in synaptic plasticity. *Learn. Memory*, **14**, 236–246.

Sossin, W.S. & Abrams, T.W. (2009) Evolutionary conservation of the signaling proteins upstream of cyclic AMP-dependent kinase and protein kinase C in gastropod mollusks. *Brain Behav. Evolut.*, **74**, 191–205.

Sutton, M.A. & Schuman, E.M. (2006) Dendritic protein synthesis, synaptic plasticity, and memory. *Cell*, **127**, 49–58.

Sutton, M.A., Ide, J., Masters, S.M. & Carew, T. (2002) Interaction between amount and pattern of training in the induction of intermediate- and long-term memory for sensitization in *Aplysia*. *Learn. Memory*, **9**, 29–40.

Wang, D.O., Kim, S.M., Zhao, Y., Hwang, H., Miura, S.K., Sossin, W.S. & Martin, K.C. (2009) Synapse- and stimulus-specific local translation during long-term neuronal plasticity. *Science*, **324**, 1536–1540.

Wong, W. & Scott, J.D. (2004) AKAP signalling complexes: focal points in space and time. *Nat. Rev. Mol. Cell Biol.*, **5**, 959–970.

Zhao, Y., Leal, K., Abi-Farah, C., Martin, K., Sossin, W. & Klein, M. (2006) Isoform specificity of PKC translocation in living *Aplysia* sensory neurons and a role for Ca^{2+}-dependent PKC APL I in the induction of intermediate-term facilitation. *J. Neurosci.*, **26**, 8847.

© 2014 Federation of European Neuroscience Societies and John Wiley & Sons Ltd